ISSN 0021-8944, Journal of Applied Mechanics and Technical Physics, 2019, Vol. 60, No. 7, pp. 1264–1277. © Pleiades Publishing, Ltd., 2019.
Russian Text © The Author(s), 2019, published in Vychislitel'naya Mekhanika Sploshnykh Sred, 2019, Vol. 11, No. 4, pp. 463–475.

Modeling of the Marangoni Instability of Uniform Diffusion through an Interface in Weightlessness Conditions

R. V. Birikh[a],*, M. O. Denisova[a],, and K. G. Kostarev[a],*****

[a] *Institute of Continuous Media Mechanics, Ural Branch, Russian Academy of Sciences, Perm, 614013 Russia*

**e-mail: rbirikh@mail.ru*

***e-mail: mod@icmm.ru*

****e-mail: kostarev@icmm.ru*

Received October 23, 2018; revised December 14, 2018; accepted December 18, 2018

Abstract—The surfactant diffusion through the vertical interface in a system of two immiscible liquids filling a horizontal channel has been studied in a two-dimensional formulation. The densities of the base liquids were initially set equal to the surfactant density. Therefore, all the subsequent density variations in the system are determined only by the contraction effect. Under nonunifrom diffusion the interfacial tension is a function of the local surfactant concentration, which gives rise to Marangoni convection. Since there are uncontrolled surface-active impurities in the system, the capillary motion is initiated in a threshold manner. It is shown that at the initial stage, despite the presence of gravity, the Marangoni convection is in the form of a series of periodically emerging paired vortices located symmetrically relative to the channel axis (as in weightlessness conditions). As the vertical density difference in the channel increases, the number of vortex pairs is reduced to one. A full-scale experiment, during which the structure of the flows and surfactant concentration fields near the interface was visualized, has been performed to verify the results of numerical simulations. The dynamics of the oscillatory mode of convection has been studied. The results of the numerical and full-scale experiments have been shown to be in qualitative agreement. The pattern of the surfactant concentration fields and stream functions in the channel as well as the time dependence of the maximum value of the stream function are presented for several values of the Marangoni and Grashof numbers. It has been found that at sufficiently large Marangoni numbers ($\mathrm{Ma} \geq 50\,000$) the diffusion process gives rise to instability in the system of immiscible liquids and a soluble surfactant, provided that their densities are equal, even in the absence of contraction.

Keywords: surfactant, interface, diffusion, weightlessness simulations, contraction, Marangoni convection, oscillatory mode.

DOI: 10.1134/S0021894419070034

1. INTRODUCTION

The main problem of laboratory simulations of hydrodynamic processes in weightlessness conditions is the impossibility to completely get rid of the influence of gravity. In this case, the Grashof number $\mathrm{Gr} = g\Delta\rho h^3/\rho_0\nu^2$, where g is the acceleration of gravity, $\Delta\rho$ is the characteristic density difference in a liquid or a system of liquids, h is the vertical size of the liquid volume, ρ_0 is the initial density of the liquids in the system, and ν is the kinematic viscosity, is traditionally taken as a basis [1–3]. The change of two parameters is used in most cases: $\Delta\rho$ in hydrostatic problems and h in convective problems.

Reducing the density difference of the liquids in a system allows the shape and behavior of liquid volumes to be estimated in microgravity conditions. Such an approach (hydro-weightlessness) was first applied by J. Plateau in 1840 when studying the shape of droplets in a rotating liquid [4]. A vertical density gradient, at which the droplet itself finds the position of equal density, is mainly created to implement this approach [5, 6]. It should be noted that the attainment of a density equal to that of the surrounding medium by the droplet does not impede the onset of gravitational convection within the droplet itself if a liquid with a density different from the density of other components of the system diffuses through the interface. In particular, the "turnover" of a droplet of a two-component mixture suspended in a den-

sity-stratified solution is explained precisely by the development of Rayleigh–Taylor instability due to diffusion [7].

A decrease in vertical size h allows the intensity of gravitational convection to be effectively influenced while keeping all of the other physical-chemical properties of the medium unchanged. However, it should be remembered that in an experiment it is possible to reduce the Grashof number by varying h only to a certain limit. This limit is determined by both the resolving power of the experimental setup and the necessity of keeping the ratio of the regions of dominance of gravitational and capillary (or different one unrelated to gravity) convection constant. The violation of the latter condition will lead the modeling to the loss of adequacy.

At the time, to simulate the microgravity conditions, attempts were made to select other parameters. For example, in [8] it was proposed to use the Morton number $\mathrm{Mo} = \eta^4 g/\rho_0\sigma_0^3$, where σ_0 is the surface tension and η is the dynamic viscosity, as a dimensionless parameter. In this case, to achieve the similarity of two non-isothermal hydrodynamic processes, the equality of the corresponding numbers serves as a necessary and sufficient condition: Mo, $\beta\Delta T$, $\sigma_T\Delta T$, Pr, and Sc, where β and σ_T are the thermal expansion and surface tension change coefficients, while Pr and Sc are the Prandtl and Schmidt numbers. However, the basic idea of this approach, i.e., the replacement of the working liquid from a space experiment by another one corresponding to ground-based modeling in changed temperature conditions, is unrealizable in practice in view of the absence of pairs of liquids with equal values of Pr and Sc.

The approach proposed in [9] is also questioned due to the large number of similarity criteria used, including the physical-chemical properties of liquids. In contrast, the dynamic Bond number $\mathrm{Bo} = \mathrm{Ra}/\mathrm{Ma}$, where Ra and Ma are the Rayleigh and Marangoni numbers, has been successfully applied to describe the interaction of free, thermo- [10], and concentration-capillary [11] convections under various gravity conditions. However, this approach also turns out to be limited, given the threshold onset of Marangoni convection in real conditions due to the presence of uncontrolled surface-active impurities [12]. In this case, retaining the Grashof number as a similarity criterion looks optimal.

Recently (see [13]), an additional way of reducing the Grashof number has been proposed for diffusion problems in a system of immiscible liquids. It consists in initially setting the densities of the base liquids on both sides of the interface equal to the diffusing liquid density. All of the subsequent density variations in this situation are connected only with the contraction effect, whose essence is a non-additive change of the volume as a result of the absorption or diffusion of one of the system's components or the phase transition made by the system. A change in the intermolecular distance and the formation of a spatial structure (as the system's state changes) or the "repacking" of molecules of the liquid mixture base component when the second component appears or disappears serve as a cause of contraction. As estimates show, the density differences arising from contraction can reach a value sufficient for the initiation of free convection. However, most often they are still smaller than those in the case of diffusion in a system with an initially arbitrary density of the base liquids approximately by an order of magnitude. Thus, using systems of equal-density liquids to model the hydrodynamics of microgravity may be deemed appropriate if we assume the Grashof number to be sufficiently small and require a geometrical similarity of the systems and an equality of the corresponding Marangoni and Schmidt numbers, because the ratio of the viscous and diffusion times becomes significant in nonstationary conditions. The goal of this paper is to illustrate the capabilities of this approach.

2. MATHEMATICAL MODEL

Consider the two-dimensional problem of concentration convection in a plane channel (L and h are the channel length and height) filled with a homogeneous liquid. A droplet of another liquid insoluble in the main liquid (droplet width d), which completely covers the channel and contains a surfactant, is placed at one of its ends. In the experiment presented below the channel was filled with an aqueous solution of sodium chloride (base liquid 1). A mixture of chlorobenzene and benzene (base liquid 2) as well as acetic acid was used to create the droplet. The densities of the base liquids were set equal to the acid density ρ_0. The acid possesses the lowest surface tension with respect to these liquids and, therefore, is a surfactant for them. The surface tension under nonuniform diffusion is a function of acetic acid concentration c, $\sigma = \sigma_0 - \sigma_1 c$ (here, σ_0 and σ_1 are the interfacial tension and the concentration coefficient of its change) and may turn out to be responsible for the liquid motion (Marangoni convection). For the simplicity of

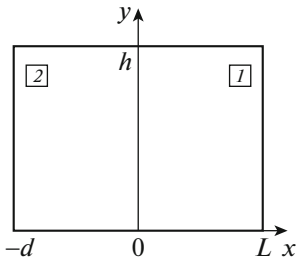

Fig. 1. Geometry of the region: *1* is the channel filled with base liquid 1; *2* is the droplet.

our numerical model, we assume that the boundary between the liquid in the channel and the droplet is flat. The geometry of the region is shown in Fig. 1.

The system of liquids is peculiar in that the base liquids are virtually insoluble in each other and would keep the density constant in the process of extraction and dissolution of the acid were it not for the contraction effect. To a first approximation, this change in density may be assumed to be proportional to the change in surfactant concentration: $\rho = \rho_0(1 - \beta^{(i)}\Delta c)$, where $\beta^{(i)}$ are the "volume expansion" coefficients of the liquids related to the contraction effect.

As our experiment showed, acid diffusion from the ternary mixture leads to a temporary increase in the density of the forming "depleted" (binary) mixture, i.e., the acetic acid in its equation of motion may be considered as a light impurity. The acetic acid dissolution in water and aqueous solutions is accompanied by positive contraction and, hence, for the liquid in channel *1* the acetic acid in the convection equations should be considered as a heavy impurity. Accordingly, the density nonuniformity resulting from contraction leads to the development of gravitational convection both in the droplet and in the channel in the gravity field.

The complete system of free convection equations in the Boussinesq approximation in dimensionless variables "stream function ψ, vorticity φ, and concentration c" is [14]

$$\frac{\partial\varphi^{(i)}}{\partial t} + \frac{\partial\psi^{(i)}}{\partial y}\frac{\partial\varphi^{(i)}}{\partial x} - \frac{\partial\psi^{(i)}}{\partial x}\frac{\partial\varphi^{(i)}}{\partial y} = \nu_i\Delta\varphi^{(i)} - \mathrm{Gr}_i\frac{\partial c^{(i)}}{\partial x}, \quad \Delta\psi^{(i)} = -\varphi^{(i)} \quad (i = 1,2),$$

$$\frac{\partial c^{(i)}}{\partial t} + \frac{\partial\psi^{(i)}}{\partial y}\frac{\partial c^{(i)}}{\partial x} - \frac{\partial\psi^{(i)}}{\partial x}\frac{\partial c^{(i)}}{\partial y} = D_i\mathrm{Sc}^{-1}\Delta c^{(i)} \quad (i = 1,2), \tag{1}$$

$$\mathrm{Gr}_i = g\beta^{(i)}C_0h^3\big/(\nu^{(1)})^2, \quad \mathrm{Sc} = \nu^{(1)}\big/D^{(1)},$$

$$\nu_1 = 1, \quad \nu_2 = \nu^{(2)}\big/\nu^{(1)}, \quad D_1 = 1, \quad D_2 = D^{(2)}\big/D^{(1)}.$$

Here, $\mathrm{Gr}_1 \le 0$, $\mathrm{Gr}_2 \ge 0$ and Sc are the Grashof and Schmidt numbers; C_0 is the maximum surfactant concentration in the initial state; $\nu^{(i)}$ and $D^{(i)}$ are the kinematic viscosities and diffusion coefficients of the liquids. As units of measurement we take: h for the distance, $h^2\big/\nu^{(1)}$ for the time, $\nu^{(1)}$ for the stream function, and C_0 for the concentration. In weightlessness conditions the Grashof numbers should be set equal to zero when describing the convection.

Let us discuss the boundary conditions. We assume the upper, lower, and left boundaries of the channel to be solid and impermeable to the material:

$$x = -d: \quad \psi = 0, \quad \frac{\partial\psi}{\partial x} = 0, \quad \frac{\partial c}{\partial x} = 0; \tag{2}$$

$$y = 0,1: \quad \psi = 0, \quad \frac{\partial\psi}{\partial y} = 0, \quad \frac{\partial c}{\partial y} = 0. \tag{3}$$

The right boundary of the liquid in the channel in our experiment is in contact with the large volume of the sodium chloride solution. Therefore, we will set the following conditions at this boundary:

$$x = L: \quad \psi = 0, \quad \varphi = 0, \quad c = 0. \tag{4}$$

We assume the interface between the liquids to be flat, impermeable to the base liquids, but admit that there is a diffusion flux of the surfactant (in our experiment the acetic acid that dissolves without limit in the aqueous solution) through it:

$$x = 0: \quad \psi_i = 0, \quad c_i = c_2, \quad D_1 \frac{\partial c_1}{\partial x} = D_2 \frac{\partial c_2}{\partial x}. \tag{5}$$

In the adopted model we assume that there is a film of uncontrolled surface-active impurities at the interface that hinders its motion. The capillary force related to the soluble surfactant concentration gradient emerging during nonuniform diffusion and the viscous stresses at the interface try to set it in motion and this will happen when the sum of these forces will exceed the threshold value P_0 characterizing the strength of the surface film in some place. Thereafter, the film is destroyed and the tangential velocity of the interface becomes nonzero, which gives rise to a flow whereby the capillary force is again balanced by the viscous stresses. Let us write the boundary and initial conditions corresponding to what is going on:

for the stationary boundary

$$x = 0: \quad \frac{\partial \psi_1}{\partial x} = \frac{\partial \psi_2}{\partial x} = 0 \tag{6a}$$

with the expression controlling the boundary immobility

$$\left| \varphi^{(1)} - \eta_2 \varphi^{(2)} + \mathrm{Ma} \times \mathrm{Sc}^{-1} \frac{\partial c}{\partial y} \right| < P_0; \tag{6b}$$

for the moving interface

$$x = 0: \quad \frac{\partial \psi_1}{\partial x} = \frac{\partial \psi_2}{\partial x}, \tag{7a}$$

$$\varphi^{(1)} - \eta_2 \varphi^{(2)} = \mathrm{Ma} \times \mathrm{Sc}^{-1} \frac{\partial c}{\partial y}. \tag{7b}$$

Here, Ma is the Marangoni number, $\mathrm{Ma} = -\dfrac{d\sigma}{dc} \dfrac{C_0 h}{\eta^{(1)} D^{(1)}}$; $\eta_2 = \eta^{(2)} / \eta^{(1)}$, where $\eta^{(1)}$ and $\eta^{(2)}$ are the dynamic viscosities of the liquids. In this case, Eq. (7b) differs fundamentally from Eq. (6b), which shows the possibility of surface film destruction when the capillary force in some place has the same direction with the viscous force (though their directions are determined by different factors), while Eq. (7b) describes the balance of the viscous stress and capillary force, which always takes place at a free boundary;

–the absence of foreign uncontrolled impurities at the interface is taken into account as $P_0 = 0$ and the condition (7b) is used in this case;

–at the initial time the liquids are at rest; in region *1* (see Fig. 1) there is no surfactant; in droplet *2* the concentration of the soluble surfactant is everywhere the same and is equal to 1 in dimensionless form:

$$t = 0: \quad \psi = 0, \quad \varphi = 0, \quad c^{(1)} = 0, \quad c^{(2)} = 1.$$

3. NUMERICAL PROCEDURE

The formulated nonstationary boundary-value problem (1)–(7) was solved by the finite difference method in regions *1* and *2* on 40×40 square grids using the implicit Crank–Nicholson scheme for equations with a time derivative. The Poisson equation for the stream function was solved by the successive over-relaxation method. We abandoned the geometrical similarity (in our calculations we assumed that $d = L = 1$) with the experiment described below, because the computation time increased very much (by more than a factor of 20 when retaining the similarity). The goal of our numerical experiment was a qualitative determination of the possible convection modes at small Grashof numbers.

The initial condition for the surfactant concentration in region *2* in our numerical computations was replaced with a smoother condition:

$$t = 0: \quad c^{(2)}_{i,k} = 1 - \exp(-10\, i / I_m),$$

where I_m is the maximum grid point number in coordinate x in region *2*. The chosen coefficient in the exponential imparts a sufficiently rapid increase in the surfactant concentration as one recedes from the interface.

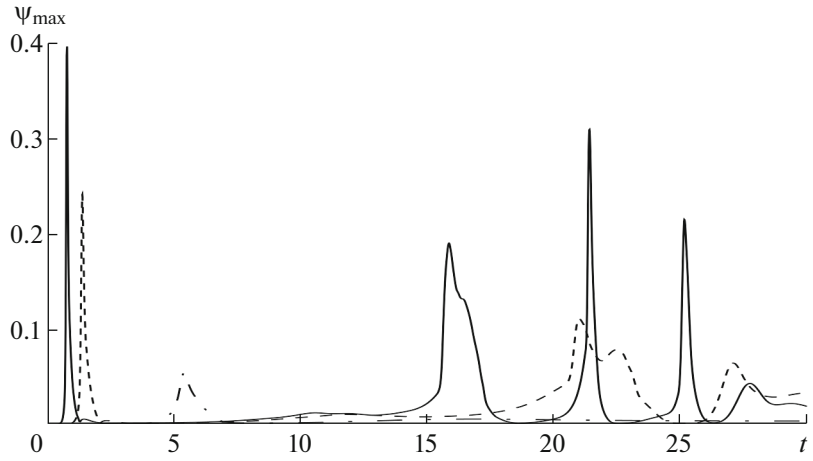

Fig. 2. Maximum value of the stream function in the droplet versus time for $Gr_1 = 0$, $Gr_2 = 0$, $P_0 = 0$, and various values of the number Ma: 1×10^5 (dash-dotted line), 3×10^5 (dashed line), and 5×10^5 (solid line).

The dimensionless parameters of the problem were close to the experimental ones: $\nu_2 = 0.53$; $\eta_2 = 0.53$; $D_2 = 1.6$; $Sc = 1250$, $Gr_1 = -50$, $Gr_2 = 50$, $P_0 = 0.10$. The Marangoni number varied from 10^3 to 5×10^5.

4. RESULTS OF THE NUMERICAL EXPERIMENT

In the first numerical experiments the diffusion process was studied in the absence of contraction, i.e., at zero Grashof numbers. At $P_0 \neq 0$ uniform surfactant diffusion was observed in the range of Marangoni numbers under consideration and no liquid motion arose. At $P_0 = 0$ and Marangoni numbers greater than 50 000 the uniform diffusion became unstable at some instant of time: a surfactant concentration gradient appeared along the interface between the liquids, which was followed by Marangoni convection. The time dependence of the intensity of liquid motion in the droplet (the maximum value of the stream function) for three Marangoni numbers is shown in Fig. 2.

For $Ma = 5\times10^5$ the first "outburst" of Marangoni convection occurs at $t = 0.4$ and lasts until $t = 1.2$. Thereafter, slow motion by inertia is observed until the nearly uniform diffusion again becomes unstable, while at $t = 15.5$ the second cycle of Marangoni convection develops. Thus, the time between the first two outbursts of Marangoni convection in the absence of gravitational convection is ~15 dimensional time units.

Figure 3 shows how the structure of the motion changes with time. The liquid motion both in the channel and in the droplet is attributable to the motion of the interface and has the same structure with a very close intensity. A significant change in the structure of the motion follows after the second outburst of Marangoni convection. There is a transition from the motion in the form of two pairs of matched vortices to one pair executing small oscillations along the interface between the regions.

Consider the influence of contraction on the diffusion process. First let us analyze the flow in the absence of a film of uncontrolled impurities ($P_0 = 0$). The gravitational convective motion arises immediately, as soon as the diffusion process begins. The density of the liquids on both sides of the interface becomes higher than the density in the remaining volume; clockwise and counterclockwise motion begins in the droplet and the channel, respectively. As a result, a vertical surfactant gradient is created, which leads to Marangoni convection. The flow intensity in the droplet at $Gr_2 = 50$ for various Marangoni numbers is presented in Fig. 4.

In the case under discussion, Marangoni convection in the lower part of the interface maintains gravitational convection through an increase in the intensity of the lower pair of vortices and decelerates the motion in the upper part of the channel. The convective flow structure and the surfactant concentration distribution are shown in Fig. 5. As can be seen, a vertical density stratification of the liquid is formed in

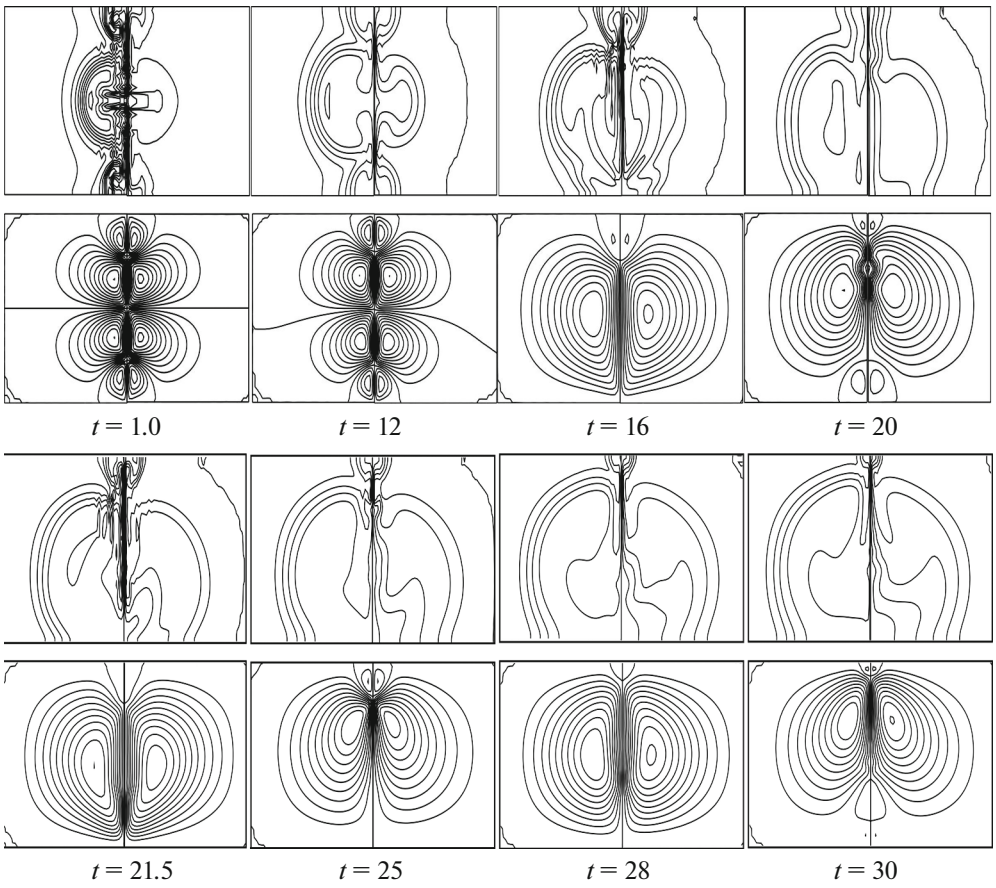

Fig. 3. Isolines of the surfactant concentration (upper row) and isolines of the stream function (lower row) at the specified instants of time for $\mathrm{Ma} = 5\times10^5$, $\mathrm{Gr}_1 = 0$, $\mathrm{Gr}_2 = 0$, $P_0 = 0$.

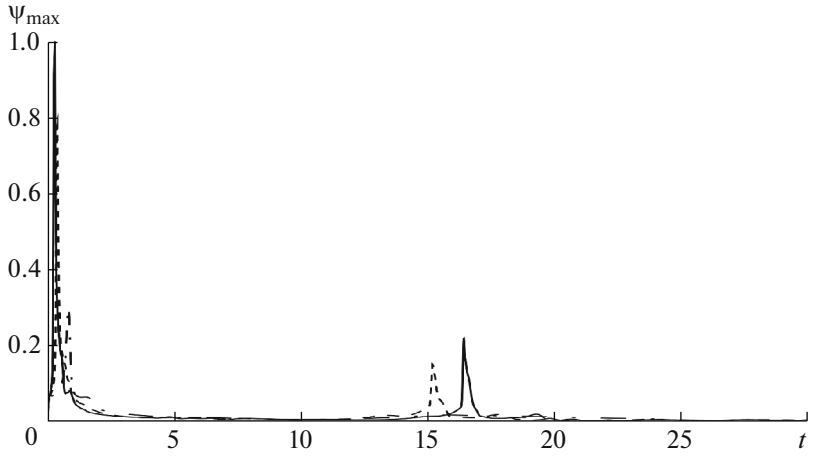

Fig. 4. Maximum value of the stream function in the droplet versus time for $\mathrm{Gr}_1 = -50$, $\mathrm{Gr}_2 = 50$, $P_0 = 0$, and various values of the number Ma: 1×10^5 (dashed-dotted line), 3×10^5 (dashed line), and 5×10^5 (solid line).

the case of an intense convective flow in the channel and the droplet and the motion slows down until the onset of diffusion instability at $t \sim 12$, as a result of which intense Marangoni convection develops ($t = 16$). Several more outbursts of this convection are observed subsequently, for example, at $t = 20$, but they are much less intense.

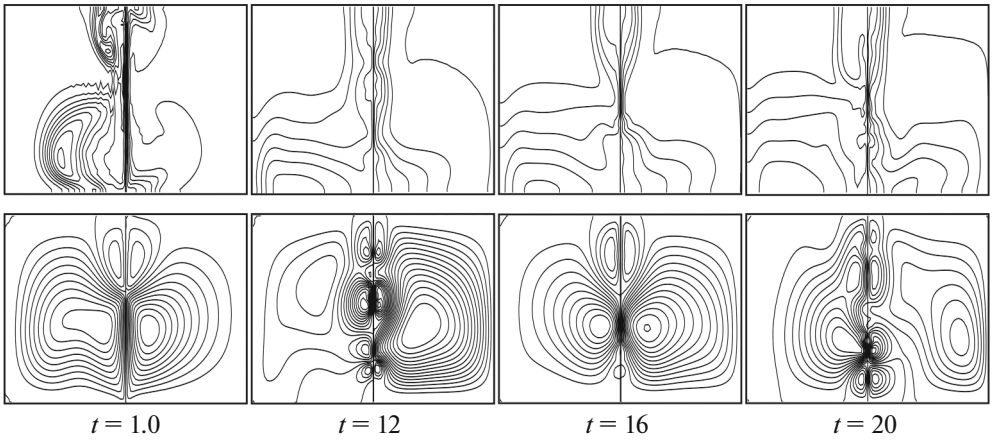

Fig. 5. Isolines of the concentration (upper row) and isolines of the stream function (lower row) at various instants of time for $\mathrm{Ma} = 5\times10^5$, $\mathrm{Gr}_1 = -50$, $\mathrm{Gr}_2 = 50$, $P_0 = 0$.

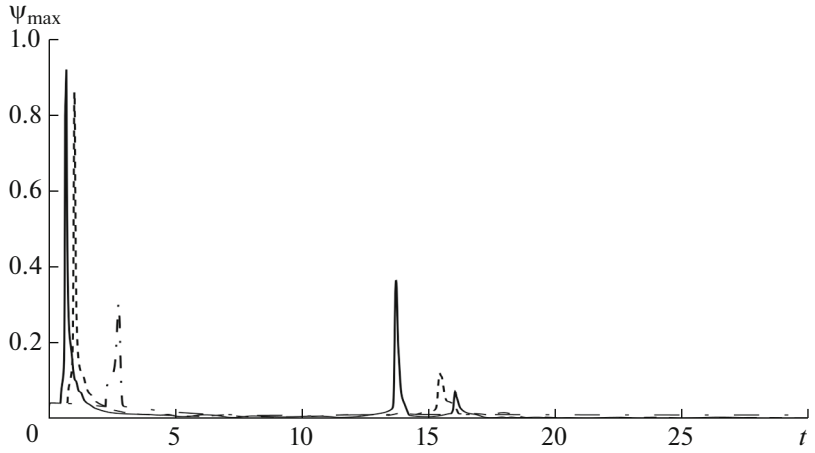

Fig. 6. Maximum value of the stream function in the droplet versus time for $\mathrm{Gr}_1 = -50$, $\mathrm{Gr}_2 = 50$, $P_0 = 10$, and various values of the number Ma: 1×10^5 (dash-dotted line), 3×10^5 (dashed line), and 5×10^5 (solid line).

Next consider the development of diffusion and convective motion when there is a film of insoluble impurities impeding the motion at the interface. Our calculations were performed for a limiting value of the parameter $P_0 = 10$, which, recall, characterizes the strength of the surface film of impurities. As our calculations showed, this limiting stress is reached at $\mathrm{Ma} = 5\times10^5$ at $t = 0.5$. Until this time the film was assumed to be solid and no convective motion was conveyed through the interface. Subsequently, intense Marangoni convection develops and a vertical density stratification decelerating the motion is formed. The change in the intensity of motion with time in the droplet is demonstrated by Fig. 6. The second outburst of Marangoni convection occurs at $t = 14$ and it is much less intense. The interval between these outbursts of convection is ~13.5 time units.

The case under consideration differs from the previous one, where there was no Bingham film at the interface between the liquids, in that the vertical stratification is formed more slowly and, as a consequence, the outbursts of concentration-capillary convection are intensified. The structure of the convective motion and the surfactant distribution in the droplet and the channel are shown in Fig. 7. Marangoni convection is presented on the frames corresponding to $t = 1$, 14, and 20.

Our calculations showed that at sufficiently large Marangoni numbers ($\mathrm{Ma} \geq 50\,000$) the diffusion process leads to the development of instability in the system of immiscible liquids and a soluble surfactant, provided that their densities are equal, even in the absence of contraction. The emerging capillary motion

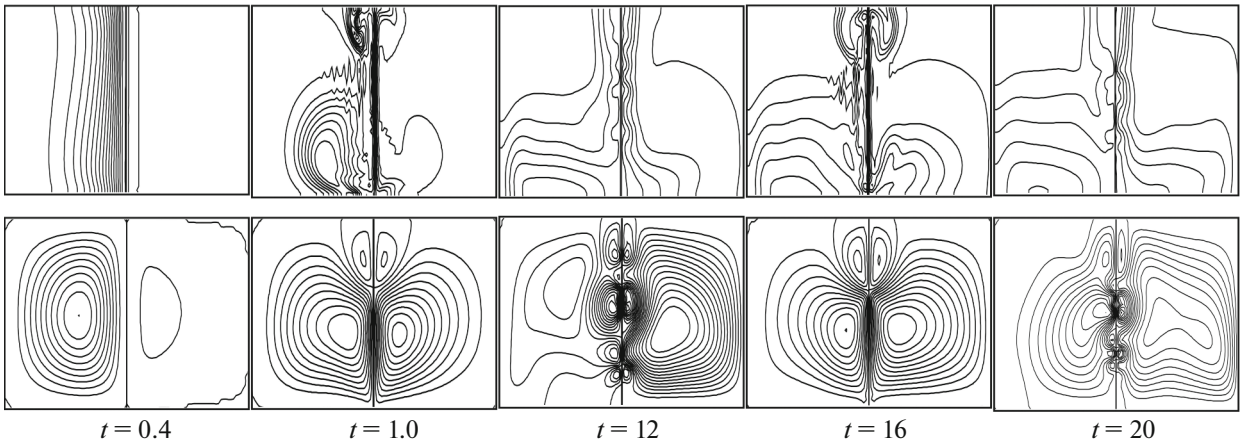

Fig. 7. Isolines of the concentration (upper row) and isolines of the stream function (lower row) at various instants of time for $\mathrm{Ma} = 5\times10^5$, $\mathrm{Gr}_1 = -50$, $\mathrm{Gr}_2 = 50$, $P_0 = 10$.

is oscillatory in pattern and has the same structure with a very close intensity of motion on both sides of the interface. Contraction in the absence of a film of insoluble surface-active impurities immediately leads to an outburst of intense Marangoni convection, with the second outburst of capillary motion being determined by the instability of uniform diffusion at large Ma. Approaching the real conditions of a physical experiment (the presence of a film of impurities) gives rise to steep surfactant concentration gradients in both regions and only afterwards does it lead to the threshold onset of capillary convection in them.

5. TECHNIQUE OF THE LABORATORY EXPERIMENT

The goal of the full-scale experiment was to solve two problems: to verify the results of our numerical simulations and to assess the role of contraction in the development of convective motion near the interface.

Let us consider the contraction effect in more detail using the dissolution of acetic acid in water as an example. In Fig. 8a the tabular and calculated (in the case of additive mixing) densities of the acid solution are plotted against the acid mass concentration. The change in intermolecular distance due to the "repacking" of molecules and the formation/destruction of a "coat" from molecules of one component around molecules of the other component in the solution as the concentration of one of the components changes, for example, during the absorption or dissolution processes, is responsible for the observed discrepancy (Fig. 8b). Since the intermolecular interaction underlies the contraction effect, the characteristic time it takes for the equilibrium (tabular) densities to be established is tens of hours, which is longer than the characteristic lifetime of the convective motion arising under diffusion from a finite liquid mixture volume by hundreds of times. Accordingly, the question of how strongly the contraction effect actually influences on the development of convection under diffusion remains open.

We experimentally studied the development of convection caused by the diffusion of a surfactant in a system of liquids with initially equal densities in a horizontal channel with a vertical interface. As the base (contacting) liquids we used a mixture of benzene and chlorobenzene (base liquid 2) and an aqueous solution of sodium chloride (base liquid 1). The initial densities of the base liquids were equal to the density of the diffusing component whose role was fulfilled by acetic acid. The acid was initially concentrated in the binary mixture.

The acetic acid density at temperature $t = 25$°C is known [15] to be 1.042 g/mL. To reach the same density, the mass concentration of benzene in its mixture with chlorobenzene was brought to $C_{01} = 21\%$. The concentration of sodium chloride in water was $C_{02} = 7.2\%$ [15]. The densities of the working liquids were determined with a Sigma 701 KSV tensiometer.

An autocollimation Fizeau interferometer with a digital video camera connected to a computer (Fig. 9) was used to study the structure and evolution of the concentration fields and flows. To carry out our experiments, we chose a cuvette with a rectangular $75\times26\times1.4$ mm^3 cavity (Fig. 10). A horizontal channel of height 2.6 mm, width 1.4 mm, and length 36 mm was formed in the cavity by parallel glass inserts. A num-

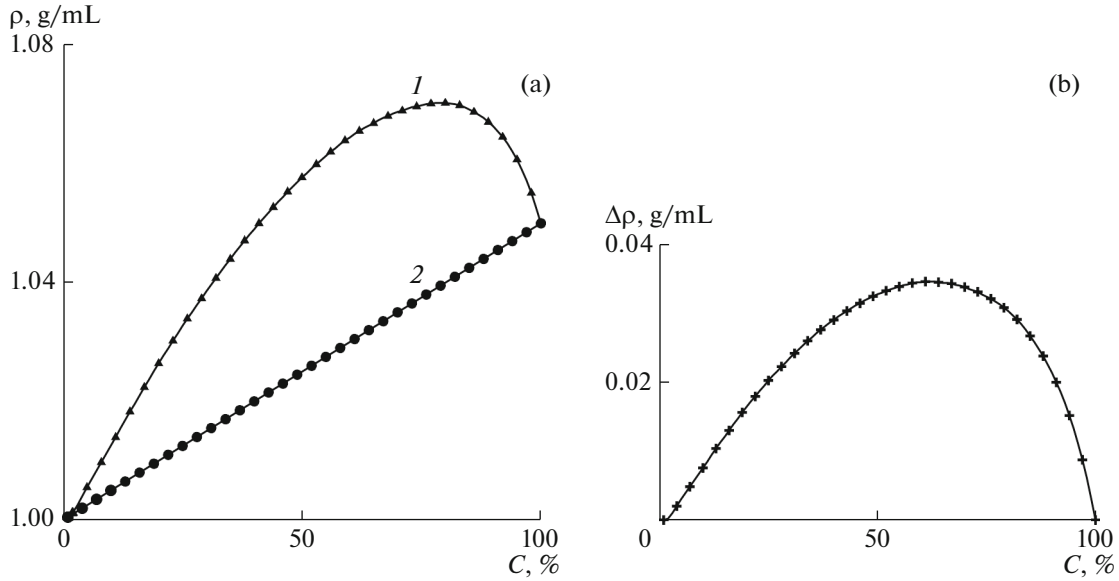

Fig. 8. (a) Acetic acid density in water versus concentration at 20°C: *1*—the tabular values [15], *2*—the calculated values under additive mixing; (b) the difference of the tabular and calculated values.

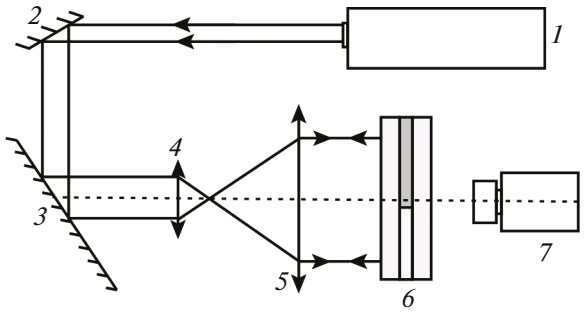

Fig. 9. Scheme of the Fizeau interferometer: *1*—helium-neon laser; *2*, *3*—turning mirrors; *4*—microlens; *5*—collimator lens; *6*—interference cuvette; *7*—video camera.

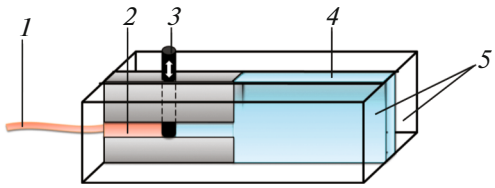

Fig. 10. Scheme of the cuvette: *1*—tube for mixture injection; *2*—mixture droplet; *3*—moving partition; *4*—solution; *5*—plane-parallel glasses (cuvette walls).

ber of holes were made in the cuvette to pour liquid 1 into and out of it and to mount a moving partition *3* to initially separate the system's liquids. The mixture droplet volume was much smaller than the solution volume (the channel was connected with a large reservoir *4*).

All our experiments were performed in accordance with the following technique. The channel was initially divided into two parts with the moving partition. A mixture containing acetic acid was poured into the left part of the channel through a tube. The right part was filled with an aqueous solution of salt, whereupon the partition was removed and the acid diffusion process began, whose dynamics was traced

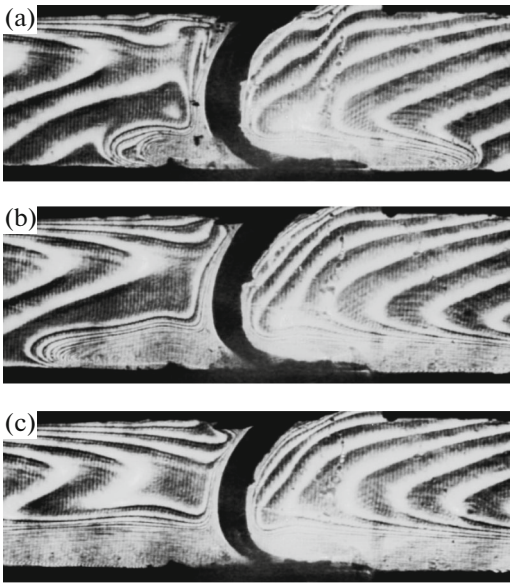

Fig. 11. Evolution of the concentration field near the interface (the mixture droplet is on the left, the aqueous solution is on the right); the initial acid concentration in the droplet $C_0 = 10\%$ at various times from the instant of droplet creation t, s: 3 (a), 13 (b), and 30 (c).

with the interferometer in real time. The experiments were conducted at an ambient temperature of (24±1)°C.

6. DESCRIPTION OF RESULTS

Owing to contraction, the acid diffusion is accompanied by a change in the density of both contacting liquids. Let us point out the peculiarities of the system chosen for our study. In particular, replacing the hydrogen atom with the chlorine atom makes chlorobenzene polar. This fact complicates significantly the formation of a homogeneous mixture of chlorobenzene and nonpolar benzene. A number of studies have revealed that the forming mixture acquires a spatial structure, while the introduction of acetic acid destroys it. As a consequence, a temporary (for several hours) increase in the volume compared to the initial one and, accordingly, a decrease in the density of the ternary mixture (there is negative contraction) is observed in the mixing process. Subsequently, the mixture returns to the original density. In contrast, the acid diffusion from the ternary mixture leads to an increase in the density of the emerging "depleted" (binary) mixture. Note that the dissolution of acetic acid in water and aqueous solutions of inorganic salts, just as in the case of ethyl alcohol, is accompanied by positive contraction.

It is well known [12] that in the presence of surface-active impurities at the interface, it starts moving only when a certain surface tension gradient created by a concentration or temperature difference is reached. Figure 11 shows a series of interferograms displaying the development of diffusion at low (subthreshold) initial acid concentrations in the droplet (the central part of the channel is presented). It is clearly seen that, in this case, the concentration isolines are parallel to the interface throughout the experiment. As a consequence of contraction, both the depleted mixture and the acid-enriched aqueous solution acquire a higher density than that in the initial state. As a result, the layers of the liquids with a changed acid concentration flow down along the interface and propagate along the channel bottom, forming a weak advective flow of gravitational nature. A maximum change in surfactant concentration and, accordingly, surface tension occurs in the meniscus region near the upper part of the channel.

The intensity of mass transfer in the system of liquids increases sharply when the concentration C_0 reaches a value exceeding the threshold one for the development of Marangoni convection (Fig. 12). The emerging capillary motion spans much of the channel, destroying the concentration distribution formed by diffusion. The competition between the intense capillary flow leveling off the nonuniform concentration distribution along the interface and the slow advective flow restoring the vertical concentration difference along it leads to the establishment of an oscillatory mode of concentration convection. The forming flow is in the form of two paired vortices and corresponds to the structure of the convective motion at

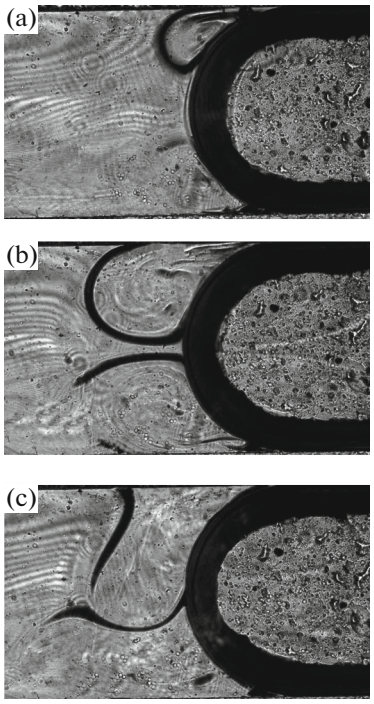

Fig. 12. Evolution of the concentration field near the interface $C_0 = 20\%$ at various times from the beginning of the Marangoni convection cycle τ, s: 1 (a), 3 (b), and 4 (c); the time from the instant of droplet creation before the beginning of the cycle is $t = 29$ s.

the initial stage in our numerical experiment for weightlessness conditions. Such a system of vortices was obtained in [16] based on the model with a surfactant surface phase in the case where the adsorption and desorption coefficients of medium 1 exceeded those of medium 2.

The "terrestrial specificity" of the dynamics of the system of liquids under study manifests itself as follows. A vertical density (and acid concentration) distribution of the base liquids resembling the one in Fig. 11c is established in the bulk of the channel immediately after the completion of the first outburst of capillary motion. As a result, the upper vortex of the next outburst of Marangoni convection develops in a mixture with a larger acid content than does the lower one and is characterized by an increase in the intensity of motion and the mass flow rate through the interface. The intensity of the latter process is so high that the acid concentration gradient between the vortex and the remaining mixture volume is perceived visually as an interface. The lower vortex is largely formed through viscous friction.

The upper vortex increases in sizes with time (Fig. 12b), gradually becomes denser than the surrounding mixture, and begins to compress the lower vortex (Fig. 12c). As a result, it cuts off the mixture flow maintaining the acid concentration difference along the interface and the capillary motion ceases, while the vortex itself slows down, settles, and frees the upper part of the interface for mixture inflow. The fresh flow touches the interface and the cycle is repeated.

To describe the oscillatory mode, let us choose the time interval between the onsets of intensification of the capillary motion in two successive cycles as a characteristic. This interval consists of two parts: the times of dominance of either capillary or gravitational convection within one cycle. The duration of the capillary and gravitational convections in different cycles of motion is illustrated by Fig. 13, from which it can be seen that the duration of the cycles is not a regular function. However, there is a clear tendency for it to increase with increasing number of oscillations through the growth of the gravitational convection time. To compare the real time in seconds with the dimensionless time used in our calculations, the former should be divided by 6.5. Since the horizontal sizes of the regions in the numerical and full-scale experiments differ significantly, it makes sense to compare the times only in the first cycle of motion, when the flow in the peripheral parts of the regions had no time to manifest itself. The duration of the first convection cycle in our experiment is about 5 s or 0.8 dimensionless time units; for the second cycle it is 11.5 s or 1.8 dimensionless time units. In the numerical model with insoluble impurities the lifetime of the first

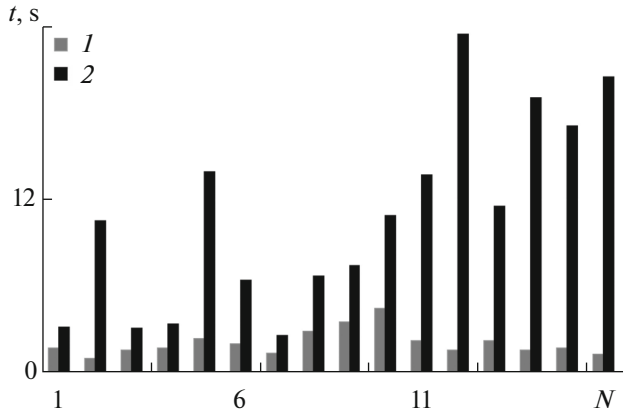

Fig. 13. Lifetime of the capillary (*1*) and gravitational (*2*) convections near the interface of the mixture with $C_0 = 20\%$ and the aqueous solution of sodium chloride with $C_{02} = 7.2\%$ versus number of cycles.

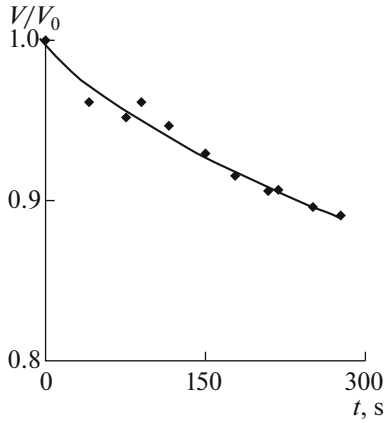

Fig. 14. Time change of the relative droplet volume in the mixture with $C_0 = 20\%$ in the acid diffusion process.

cycle is 13.5 time units. This discrepancy is thought to be a consequence of the difference in channel length during our experiment and calculations.

In the experiment the droplet volume decreases as the acid diffuses. As our measurements suggest (Fig. 14), such a change in the droplet volume with time is nearly linear. This behavior most likely stems from the fact that maximum acid diffusion occurs at the capillary stage of the cycle, with the mixture contained in the Marangoni cell volume being mainly drawn into this process. Our measurements revealed that whereas at the beginning of the oscillatory mode this cell occupies approximately 1/10 of the entire droplet volume, by the end, after the reduction in acid content in the mixture, it encloses up to 1/3 of the droplet. Given that the duration of the capillary convection changes little during the entire experiment (see Fig. 13), it can be assumed that a similar amount of acid leaves the droplet in each cycle, as confirmed by Fig. 14.

In conclusion, note that the Marangoni convection ends long before the complete acid depletion in the droplet. An analysis of the video of our experiment and the dependence shown in Fig. 14 lead us to the following conclusion: the change of modes occurs at an acid concentration of about 11% (at $t = 200$ s), which is higher than 10% — the threshold value for the system under consideration. This fact suggests that insoluble impurities accumulate at the interface during diffusion.

The measures to prepare the cuvette itself play a major role in the temporal evolution of the system of liquids. For example, the peculiarities of its design did not allow the walls to be cleaned before each experiment; the number of insoluble impurities in the cuvette increased with time. As a consequence, whereas at the beginning of the series of experiments there was a convective mode during which, as our theoretical analysis predicted, the number of vortex pairs had time to decrease to one and, thereafter, it was replaced

by a diffusive one, in the succeeding experiments the diffusive mode arose already after the stage of the convective mode, at which two pairs of cells were present.

Within our main experiment we also performed a series of additional measurements to elucidate the causes of the development of intense convection in the chosen system of liquids. It particular, we found that sodium chloride added to water to achieve the equality between the initial densities of the system's liquids did not change, contrary to expectation, the form of the concentration dependence of the solution density, i.e, $\partial\rho/\partial C$ remains as before. Given this fact, we attempted to use a bell-shaped form of the concentration dependence of the acid solution density (see Fig. 8a), for which purpose the solution of neutral salt was replaced by an aqueous solution of acid. The experiment turned out to be fruitless, because the acid content in both contacting liquids should be increased sharply to pass into the region of necessary concentrations. However, the mutual solubility of the base liquids increases with leading rates as the acid concentration grows; near $C_0 = 50\%$ the interface disappears and a significantly inhomogeneous three-component solution is formed.

7. CONCLUSIONS

The diffusion of a surfactant in a system of liquids with equal initial densities and a vertical interface was studied experimentally and theoretically. The contraction effect accompanying the change in surfactant concentration on both sides of the interface was found to generate local liquid density nonuniformities and to produce gravitational convection. However, these density differences, at least in one of the liquids, remain smaller than those in a system based on single-component liquids by an order of magnitude.

The capillary motion in the chosen system of liquids was shown to arise in a threshold way, with the final concentration flow acquiring an oscillatory pattern. The structure of the flow and its evolution are qualitatively confirmed by our numerical simulations of the diffusion in systems with contraction and Bingham behavior of the interface in microgravity conditions.

REFERENCES

1. *Konvektivnye protsessy v nevesomosti* (Convective Processes in Microgravity), Polezhaev, V.I., Ed., Moscow: Nauka, 1991.
2. Bogatyrev, G.P., Ermakov, M.K., Ivanov, A.I., Nikitin, S.A., Pavlovskii, D.S., Polezhaev, V.I., Putin, G.F., and Savin, S.F., Experimental and theoretical investigation of thermal convection in a terrestrial model of a convection detector, *Fluid Dyn.,* 1994, vol. 29, pp. 645–652. https://doi.org/10.1007/BF02030492
3. *Physics of Fluids in Microgravity*, Monti, R., Ed.,London: Taylor, 2001.
4. Plateau, J., Experimental and theoretical researches on the figures of equilibrium of a liquid mass withdrawn from the actions of gravity, *Annual Report of the Board of Regents of the Smithsonian Institution,* Washington, DC: Government Printing Office, 1864, pp. 207–285.
5. Kosvintsev, S.R. and Reshetnikov, D.G., Drop motion induced by diffusion of soluble surfactant the external medium: Experiment, *Colloid J.,* 2001, vol. 63, pp. 318–325. https://doi.org/10.1023/A:1016648311449
6. Morozov, K.I. and Lebedev, A.V., Bifurcations of the shape of a magnetic fluid droplet in a rotating magnetic field, *J. Exp. Theor. Phys.,* 2000, vol. 91, pp. 1029–1032. https://doi.org/10.1134/1.1334993
7. Kostarev, K.G. and Briskman, V.A., Dissolution of a drop with a content of a surface-active substance, *Dokl. Phys.,* 2001, vol. 46, pp. 349–351. https://doi.org/10.1134/1.1378101
8. Volkov, P.K., Similarity in problems related to zero-gravity hydromechanics, *Phys.–Usp.,* 1998, vol. 41, pp. 1211–1217. https://doi.org/10.1070/PU1998v041n12ABEH000513
9. Andreyev, V.K., Gaponenko, Yu.A., Goncharova, O.N., and Pukhnachev, V.V., *Sovremennyye matematicheskie modeli konvektsii* (Advanced Mathematical Models of Convection), Moscow: Fizmatlit, 2008.
10. Mizev, A.I. and Schwabe, D., Convective instabilities in liquid layers with free upper surface under the action of an inclined temperature gradient, *Phys. Fluids,* 2009, vol. 21, 112102. https://doi.org/10.1063/1.3251755
11. Mizev, A. and Birikh, R., Interaction between buoyant and solutocapillary convections induced by a surface-active source placed under the free surface, *Eur. Phys. J. Spec. Top.,* 2011, vol. 192, pp. 145–153. https://doi.org/10.1140/epjst/e2011-01369-3

12. Mizev, A., Denisova, M., Kostarev, K., Birikh, R., and Viviani, A., Threshold onset of Marangoni convection in narrow channels, *Eur. Phys. J. Spec. Top.,* 2011, vol. 192, pp. 163–173. https://doi.org/10.1140/epjst/e2011-01371-9
13. Denisova, M.O., Kostarev, K.G., Oshmarina, M.V., Torokhova, S.V., Shmyrov, A.V., and Shmyrova, A.I., Contraction in nonequilibrium fluid systems, in *Neravnovesnye protsessy v sploshnykh sredakh. Materialy mezhdunar. simpoziuma* (Proceedings of the International Symposium on Non-Equilibrium Processes in Continuous Media, Perm, May 15–18, 2017), Perm': Permsk. Gos. Nats. Issled. Univ., 2017, vol. 1, pp. 152–155.
14. Birikh, R.V., Briskman, V.A., Velarde, M.G., and Legros, J.-C., *Liquid Interfacial Systems: Oscillations and Instability,* New York, Basel: Marcel Dekker, 2003.
15. *Spravochnik khimika* (Guide Book for Chemists), vol. 3: *Khimicheskoe ravnovesie i kinetika. Svoistva rastvorov. Elektrodnye protsessy* (Chemical Equilibrium and Kinetics. Properties of Solutions. Electrode Processes), Nikol'skii, B.P., Ed., Moscow, Leningrad: Khimiya, 1965.
16. Birikh, R.V., Stability of homogeneous non-stationary surfactant diffusion through a flat interface between liquids, *Vestn. Permsk. Univ., Fiz.,* 2016, no. 1 (32), pp. 64–70. https://doi.org/10.17072/1994-3598-2016-1-64-70

Translated by V. Astakhov